IOWA STATE UNIVERSITY
Digital Repository

Chemical and Biological Engineering Publications | Chemical and Biological Engineering

2005

A Combined Triboelectrochemical QCM for Studies of the CMP of Copper

Wenquan Lu
Iowa State University

Jian Zhang
Cabot Microelectronics

Frank Kaufman
Cabot Microelectronics

See next page for additional authors

Follow this and additional works at: http://lib.dr.iastate.edu/cbe_pubs

Part of the Chemical Engineering Commons, and the Chemistry Commons

The complete bibliographic information for this item can be found at http://lib.dr.iastate.edu/cbe_pubs/125. For information on how to cite this item, please visit http://lib.dr.iastate.edu/howtocite.html.

This Article is brought to you for free and open access by the Chemical and Biological Engineering at Iowa State University Digital Repository. It has been accepted for inclusion in Chemical and Biological Engineering Publications by an authorized administrator of Iowa State University Digital Repository. For more information, please contact digirep@iastate.edu.

A Combined Triboelectrochemical QCM for Studies of the CMP of Copper

Abstract

In order to improve our understanding of the fundamental surface processes associated with the chemical mechanical planarization ~CMP! of metals, we have developed an experimental tool that combines the high resolution mass sensing capabilities of the quartz crystal microbalance ~QCM! with a triboelectrochemical testing system. A electrochemical QCM is combined with a polishing tool and force sensor in order to perform controlled surface abrasion while simultaneously monitoring mass changes and electrochemical signals at the metal/solution interface. This system can be used to simulate a metal polishing process with in situ surface measurement capabilities. Typical parameters that can be measured include etch rates, polishing rates, and repassivation kinetics via changes in the resonance frequency of the quartz crystal before, during, and after polishing. Simultaneous measurements of electrochemical parameters, such as the electrode current or open circuit potential, provide a direct correlation between polishing parameters and electrochemical signals. The behavior of copper in various solutions illustrates the capabilities of this technique and highlights the complexities of the metal polishing process. The influence of pH, benzotriazole, peroxide, and several slurry chemistries are examined.

Disciplines

Chemical Engineering | Chemistry

Comments

This article is from *Journal of The Electrochemical Society* 152 (2005): B17-B22, doi: 10.1149/1.1836124. Posted with permission.

Authors

Wenquan Lu, Jian Zhang, Frank Kaufman, and Andrew C. Hillier

This article is available at Iowa State University Digital Repository: http://lib.dr.iastate.edu/cbe_pubs/125

Journal of The Electrochemical Society, **152** (1) B17-B22 (2005)
0013-4651/2004/152(1)/B17/6/$7.00 © The Electrochemical Society, Inc.

A Combined Triboelectrochemical QCM for Studies of the CMP of Copper

Wenquan Lu,[a,c,*] Jian Zhang,[b,] Frank Kaufman,[b,**] and Andrew C. Hillier[a,**,z]**

[a]*Department of Chemical Engineering and Department of Chemistry, Iowa State University, Ames, Iowa 50011, USA*
[b]*Cabot Microelectronics, Aurora, Illinois 60504, USA*

In order to improve our understanding of the fundamental surface processes associated with the chemical mechanical planarization (CMP) of metals, we have developed an experimental tool that combines the high resolution mass sensing capabilities of the quartz crystal microbalance (QCM) with a triboelectrochemical testing system. A electrochemical QCM is combined with a polishing tool and force sensor in order to perform controlled surface abrasion while simultaneously monitoring mass changes and electrochemical signals at the metal/solution interface. This system can be used to simulate a metal polishing process with *in situ* surface measurement capabilities. Typical parameters that can be measured include etch rates, polishing rates, and repassivation kinetics via changes in the resonance frequency of the quartz crystal before, during, and after polishing. Simultaneous measurements of electrochemical parameters, such as the electrode current or open circuit potential, provide a direct correlation between polishing parameters and electrochemical signals. The behavior of copper in various solutions illustrates the capabilities of this technique and highlights the complexities of the metal polishing process. The influence of pH, benzotriazole, peroxide, and several slurry chemistries are examined.
© 2004 The Electrochemical Society. [DOI: 10.1149/1.1836124] All rights reserved.

Manuscript submitted May 26, 2004; revised manuscript received June 7, 2004. Available electronically December 6, 2004.

Copper has become the preferred wiring material for the next generation of integrated circuits due to its high conductivity and superior electromigration resistance.[1,2] However, copper metallization techniques introduce several new technical challenges to the circuit fabrication process. In particular, the construction of copper interconnects by the dual-damascene method involves a surface planarization step with extremely strict requirements.[3,4] In dual-damascene processing, copper is electrodeposited into lines and vias. The electrodeposits are subsequently leveled by chemical mechanical planarization (CMP) to achieve a uniformly smooth and level surface.[5,6] Unfortunately, differences in removal rates of copper and the adjacent low dielectric materials result in unacceptable surface features such as dishing of copper or erosion of the dielectric material, which require additional processing steps to correct.[5,7,8] In addition, many of copper's inherent properties make control of surface topography during the various wet and dry processing steps difficult.

During the CMP process, a polishing pad is brought into contact with a surface of interest. Planarization is achieved through a combination of mechanical abrasion, chemical reaction, and electrochemical etching.[9] Input parameters that influence the planarization process include polishing force, pad material, solution conditions, and various additives that can promote the formation of surface films or accelerate/inhibit surface reactions. Given the complexities of this process and the combination of mechanical and chemical processes taking place, control of the final surface parameters is challenging. Therefore, a detailed understanding of the fundamental surface behaviors associated with copper CMP is critical in order to advance beyond a purely empirical control of this process.[4,10,11]

The electrochemistry of copper has been the subject of numerous studies and a great deal is known about its behavior.[12-14] However, only recently have attempts been made to address copper CMP in a systematic manner in an attempt to understand its complexities.[3,5-8,10,11,15-20] One of the requirements involved in creating a detailed understanding of copper CMP is the development of measurement tools that can directly elucidate changes in the metal surface during polishing. Typical measurement systems used to study metal CMP combine a surface polishing tool with an electrochemical workstation.[11,17,21] Changes in the open circuit potential (OCP) are used to monitor changes in the metal surface during polishing. Although relative changes in film thickness can be measured by several techniques *in situ*, absolute changes in film thickness can only be determined *ex situ*, which makes it difficult to accurately deduce polish or etch rates.

In order to improve the ability to monitor copper CMP processes *in situ*, we have developed a measurement tool that combines a polishing system with a quartz crystal microbalance (QCM) and an electrochemical workstation.[22,23] The resulting triboelectrochemical quartz crystal microbalance (T-EQCM) allows direct and real-time measurement of mass changes at a metal surface before, during, and after polishing. In this report, we describe experimental details of the T-EQCM system and perform proof-of-concept experiments that evaluate copper polishing. In particular, we examine the influence of polishing force, solution pH, and the addition of benzotriazole on the polishing behavior of copper films. Several simulated slurries containing polishing particles, oxidizer, and inhibitor are also examined to test real slurry chemistries.

Experimental

Reagents.—All experiments were performed using electrolytes dissolved in 18 MΩ deionized (DI) water (E-Pure, Barnstead, Dubuque, IA). Electrochemical measurements were performed in solutions containing as-received sulfuric acid, sodium sulfate, sodium hydroxide, hydrogen peroxide, and benzotriazole (BTA) (Aldrich, Milwaukee, WI). Polishing slurries (Cabot Microelectronics, Aurora, IL) consisted of alumina suspensions with different levels of pH, oxidizer (peroxide), and inhibitor (BTA).

Substrate preparation.—Substrates consisted of thin copper films deposited onto commercially available quartz crystals. Gold-coated quartz crystals (Elchema, Potsdam, NY) with a resonance frequency of 10 MHz and an electrode area of ~0.2 cm^2, were used as received. The crystals were cleaned by rinsing with ethanol and then deionized water followed by drying under nitrogen. Copper films were subsequently electroplated from a solution of 5 mM Cu_2SO_4 in 0.05 M H_2SO_4 onto the upper QCM surface by a pulsed potential waveform in which a square-wave between 0.62 and −0.46 V (*vs.* Hg/$HgSO_4$) was applied at a frequency of 500 Hz. The pulsed potential profile was chosen to improve the uniformity of deposition and decrease the copper grain size. Deposition was continued until a mass change of 90 μg, as deduced by a shift in the crystal resonance frequency, was achieved. This mass change corresponds to a copper

* Electrochemical Society Student Member.
** Electrochemical Society Active Member.
[c] Presents address: Argonne National Laboratory, Argonne, IL 60439.
[z] E-mail: hillier@iastate.edu

Downloaded on 2014-05-22 to IP 129.186.176.40 address. Redistribution subject to ECS terms of use (see ecsdl.org/site/terms_use) unless CC License in place (see abstract).

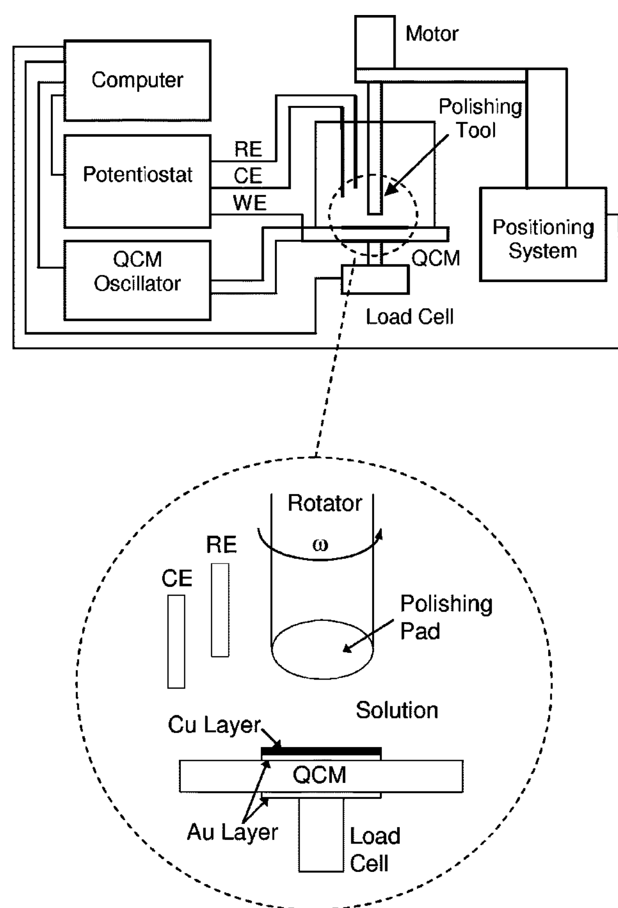

Figure 1. Schematic of T-EQCM system, including EQCM, polishing tool, positioning system, load cell, and computer with interface electronics. Inset: expanded view of sample region showing EQCM and polishing tool with copper working electrode and (CE) and reterence (RE) electrodes.

film thickness of ~0.5 μm. Calibration of the quartz crystal response provided the expected linear relationship between crystal resonance frequency and mass change, as deduced by the electrochemical charge. A calibration constant of 1.0 Hz ng^{-1} was determined for the 10 MHz crystals used here. Following deposition, the copper film was heated in an oven at 100°C for 10 min.

Surface characterization.—The topography of the copper surfaces was evaluated before and after polishing using a combination of optical microscopy and atomic force microscopy (AFM). AFM images were acquired with a commercial scanning probe microscope (Molecular Imaging, Inc., Phoenix, AZ) in contact mode powered by a Nanoscope E controller (Digital Instruments, Santa Barbara, CA). Commercially available Si_3N_4 AFM tips (Nanoprobe, Park Scientific) exhibiting a spring constant of $k \sim 0.1$ N m^{-1} were used for imaging.

Tribo-electrochemical quartz crystal microbalance.—The tribo-electrochemical quartz crystal microbalance (T-EQCM) consisted of an electrochemical quartz crystal microbalance (EQCM), a polishing tool with force sensor, a positioning system, and a computer for data acquisition and control (Fig. 1). The QCM used in this work was a commercially available system combined with a potentiostat (Elchema, Potsdam, NY). The selection of the QCM was based on a combination of fast time response (~1-5 ms), sensitivity (~0.1 Hz), and the ability to access analog output channels for coordination with a computer data acquisition and control program. The EQCM system included an oscillator circuit and frequency counter to operate at 10 MHz QCM. Changes in the crystal resonance frequency are measured with a sensitivity of ~0.1 Hz at a selectable acquisition rate between 1 ms and several seconds. The potentiostat provides electrochemical control of the upward-facing electrode surface.

The polishing tool included a voltage-controlled rotating motor, a load cell, and a three-dimensional positioning system. The rotating motor (Maxon Motors, Burlingame, CA) was mounted directly on the z axis of a positioning system. The positioning system provided three-dimensions of high resolution, computer controllable motion. A controller and motor driven unit (Newport Corporation, Irvine, CA) were combined with three integrated stepper motors/linear translation stages that offered 100 mm travel range with fast, submicrometer resolution motion. The motors were mounted directly to an optical breadboard (Newport Corporation, Irvine, CA) with an orthogonal arrangement to give three-dimensional motion. A glass rod was mounted to the shaft of the rotating motor, and a piece of commercially available polishing pad (Epic™ model A100, Cabot Microelectronics, Aurora, IL) was glued to the lower surface. The rotation rate of the motor was controlled by an externally supplied voltage. Typical rotation rates for the shaft were 1000 rpm for a 10 V input.

A magnified schematic of the interface between the quartz crystal surface and the polishing tool illustrates the important details (Fig. 1, inset). The QCM was mounted in an upward-facing Teflon cell with a lid containing holes for counter and reference electrodes as well as allowing insertion of the glass rod with polishing pad. The entire cell assembly was mounted directly on a load cell (Omega Engineering, Stamford, CT) that was used to measure and control the polishing force. Counter and reference electrodes consisted of a wound Pt/Ir wire and a $Hg/HgSO_4$ (MSE) electrode, respectively. The QCM possessed gold on titanium excitation electrodes placed on opposing crystal surfaces that allow the crystal to be vibrated at its resonance frequency. The upper electrode surface also served as the working electrode with adjacent counter and reference electrodes in a three-electrode electrochemical cell. The working electrode surface was coated with an electrodeposited copper layer (vide supra) to act as the test surface prior to measurements.

In a typical polishing experiment, solution was added to the cell and the crystal response and the OCP were allowed to stabilize. The polishing force and the substrate position were initially determined by centering the polishing rod over the crystal and slowly approaching the surface without rotation until contact occurred. Contact between the crystal and the polishing rod appeared as a change in the load force and an increase in the crystal resonant frequency. The zero position was defined as the position where the load cell and crystal frequency first changed when the surface was contacted. The load force could then be set by displacement of the rod downward into the crystal until a specified force was measured. The polishing rod was then backed away from the surface a known distance. A typical polishing experiment involved rotating the polishing rod while not in contact with the surface for a period of time, displacing the rod into the surface to a fixed load force for a determined polishing period, and then removing the polishing rod from the surface. During this process, the resonance frequency, OCP (or current), displacement, and load force were simultaneously monitored.

Results and Discussion

Examples of the surface topography associated with the polishing process on an electrodeposited copper film are shown in Fig. 2. The polishing pad creates a circular scratch pattern (Fig. 2A) whose diameter is consistent with the contact area between the pad and the copper surface. Notably, this contact area is ~0.11 cm^2, which is somewhat smaller than the active QCM electrode area of 0.2 cm^2. Higher resolution AFM images illustrate the detailed surface structure (Fig. 2B and C). Before polishing, the copper surface consists of a layer of densely packed copper grains with a peak-to-valley height of 170 nm μm^{-2} (Fig. 2B). After polishing, the surface acquires a ridged structure that conforms to the macroscopic topography of the polishing pad and the local peak-to-valley height decreases to 67 nm.

Downloaded on 2014-05-22 to IP 129.186.176.40 address. Redistribution subject to ECS terms of use (see ecsdl.org/site/terms_use) unless CC License in place (see abstract).

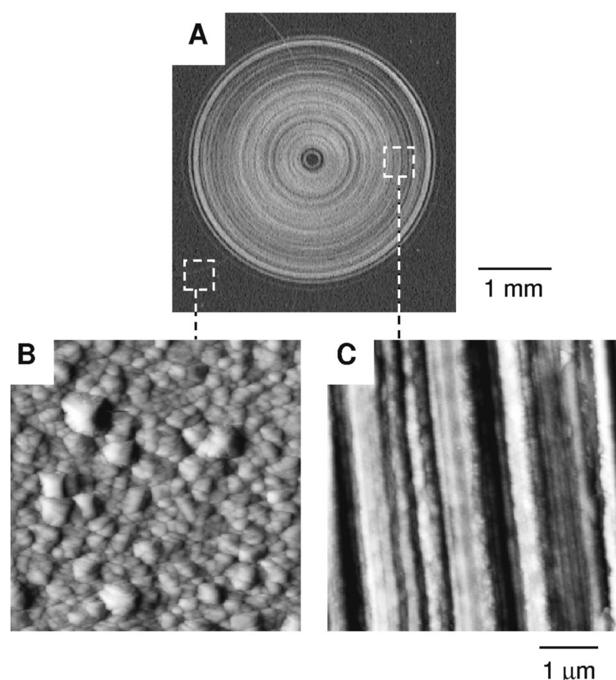

Figure 2. Images of copper film after polishing in air. (A) Optical micrograph of circular polish mark left by 3 mm diam polishing pad. (B) AFM image of unpolished region of copper. (C) AFM image of polished region of copper. The z range in the AFM images is 800 nm.

Figure 3 depicts the results from a typical polishing experiment on an electrodeposited copper film in a solution of 0.1 M Na_2SO_4 at pH 12. In this experiment, tool displacement (Fig. 3A), load force (Fig. 3B), OCP (Fig. 3C), and crystal resonance frequency (Fig. 3D) are recorded as functions of time. For the first 5 s, the polishing tool is rotated while held in solution at a separation of ~120 μm from the copper surface. At $t = 5$ s, the tool is rapidly pushed into the sample surface and held in contact for 15 s while the pad rotates.

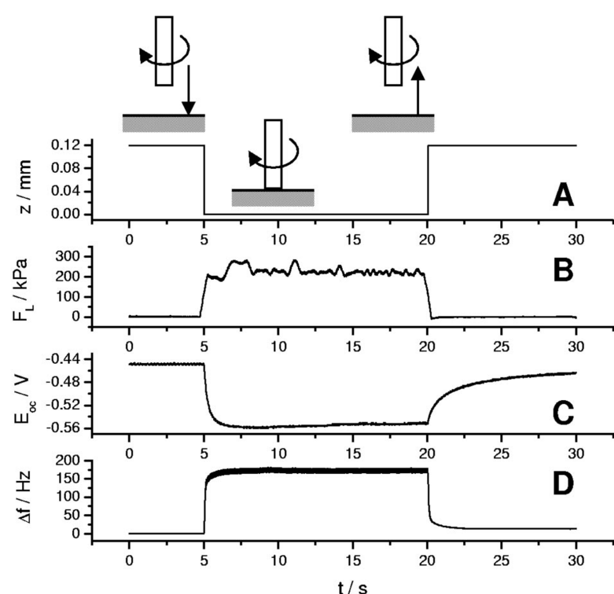

Figure 3. Summary of T-EQCM response for copper film during polishing experiment: (A) vertical position of polishing tool, (B) measured load force (F_L), (C) OCP, and (D) frequency response of EQCM during a 15 s polish in 0.1 M Na_2SO_4 at pH 12.

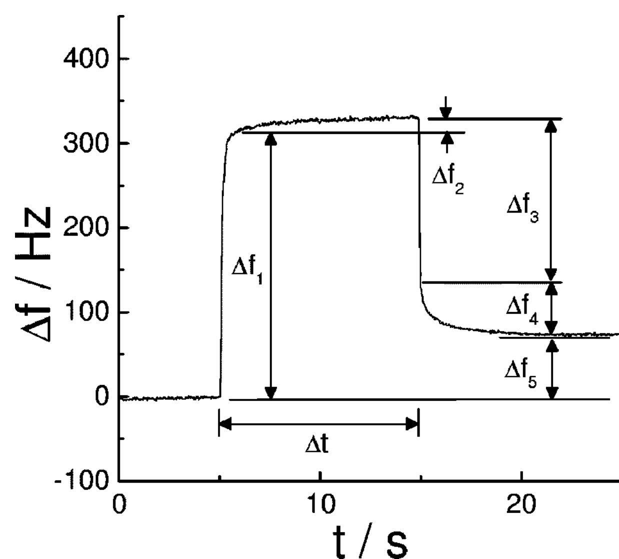

Figure 4. Summary of important frequency changes observed during typical polishing experiment. Details of the origins and interpretations of the various Δf values are described in the text.

Changes in load force, OCP, and crystal resonance frequency occur while the rotating pad contacts the surface. The load force increases to 200 kPa and remains constant until the tool is removed. Notably, the load force during polishing is selected prior to the experiment and maintained at a constant value until the tool is removed from the surface. A decrease in the OCP from an initial steady value of −0.46 V down to −0.55 V is observed as the tool contacts the surface. This decrease in potential is presumably due to the abrasive action of the polishing pad, which removes material from an oxide-coated surface and exposes copper metal. The initial open circuit value (−0.46 V) represents the oxide-coated copper, while the value during polishing (−0.55 V) results from fresh copper metal being exposed. When the tool is removed ($t = 20$ s), the OCP slowly increases back to its initial value of −0.46 V due to repassivation of the copper film.

The response of the crystal resonance frequency in Fig. 3D represents a complex combination of processes. Details of this behavior are illustrated in an expanded view of the frequency response in Fig. 4. At first contact with the polishing pad ($t = 5$ s), the crystal frequency increases in value (Δf_1). This increase is due to the downward force felt by the crystal from the polishing tool and is characteristic of a compressive stress applied to the crystal surface.[24] The magnitude of this increase in frequency is linear with applied force at small forces, but the crystal frequency plateaus to a constant value at higher forces. As polishing proceeds, the crystal frequency increases slowly in a continuous manner (Δf_2). This increase is primarily due to the mass loss associated with removal of copper from the substrate by polishing. However, the frequency can also decrease in this region as the substrate is polished. This decrease is the result of removal of material, which decreases the applied force by increasing the gap between the surface and the polishing tool. Thus, the frequency change observed during polishing is due to a competition between material removal (higher frequency) and a decreased load force (lower frequency). The frequency may increase or decrease, depending upon the relative importance of the removal rate and the change in load force. Indeed, both increases and decreases in frequency have been observed during the polishing step in various experiments. Thus, the frequency change during polishing Δf_2 cannot be simply used to infer quantitative surface changes. However, other frequency values measured before and after polishing are not affected by the variability of this process. When the polishing tool is removed from the surface at $t = 15$ s, the frequency drops instantaneously to a lower value (Δf_3). This drop

Downloaded on 2014-05-22 to IP 129.186.176.40 address. Redistribution subject to ECS terms of use (see ecsdl.org/site/terms_use) unless CC License in place (see abstract).

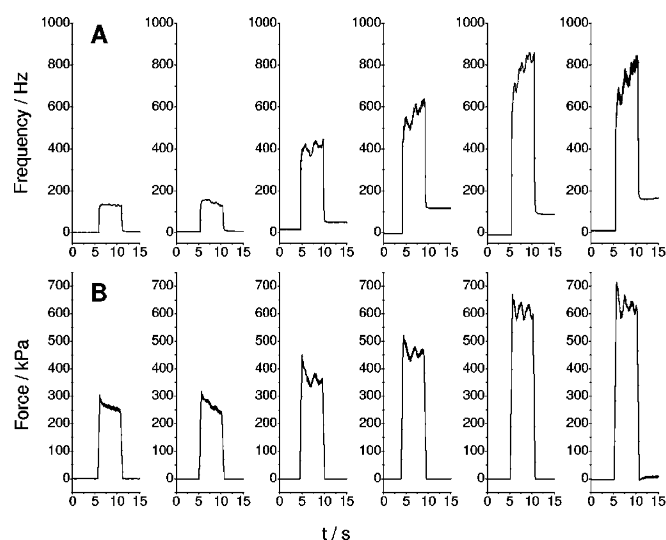

Figure 5. Polishing experiments showing frequency response and load force (F_L) as a function of increasing applied load. (A) Frequency response and (B) load force during 5 s polish of copper surface in 0.1 M Na_2SO_4 at pH 10 as a function of increasing load force.

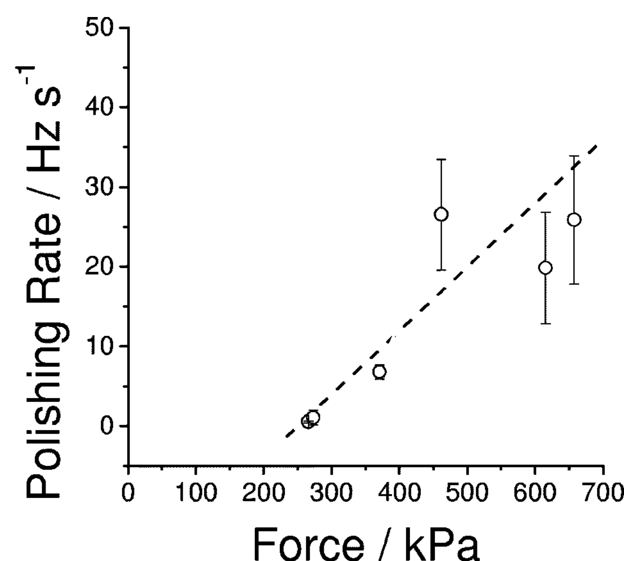

Figure 6. Summary of polishing rate data as a function of load force from Fig. 5. The line represents a straight line fit of the data with a slope of 0.058 Hz s^{-1} kPa^{-1} and a R^2 value of 0.86.

reflects a decrease in frequency due to removal of the applied force. A further, slow decrease in the crystal frequency (Δf_4) is then observed, which is attributed to a surface filming process such as the formation of an oxide layer. Similar experiments in air suggest that the crystal also exhibits a small relaxation in the absence of film formation, but this process has a time constant of less than 60 ms and, thus, is a minor component of the *in situ* results. The final frequency value attained by the crystal reflects the total change in surface mass due to polishing. In particular, the frequency change (Δf_5) provides a measure of the mass loss that occurs during polishing and can be used to determine the polishing rate ($\Delta f_5/\Delta t$).

Figures 3 and 4 illustrate that the T-EQCM technique can be used to measure a variety of dynamic processes that occur during polishing. Figure 5 depicts the results of several polishing experiments performed in 0.1 M Na_2SO_4 at pH 10. In each experiment, the polishing tool was brought into contact with the copper surface for 5 s and then removed. The frequency response and the force are recorded for increasing load force values. In each experiment, the frequency response exhibits behavior similar to that in Fig. 4. The frequency increases upon initial contact with the polishing tool to a value that is proportional to the load force. When the tool is removed, the frequency response decreases back to a magnitude that is higher than the initial value. This increase in the frequency reflects the removal of material from the copper surface due to contact with the pad.

The polishing rate for each experiment depicted in Fig. 5 can be quantified by taking the difference between the initial and final frequency value and then dividing by the polishing time. Results of a series of measurements are plotted in Fig. 6 to illustrate the influence of polishing force on polishing rate. The data reflects a linear increase in polishing rate over the forces examined. This behavior is consistent with the Preston equation[25]

$$\frac{dh}{dt} = \alpha P_L \quad [1]$$

where the polishing rate is linearly proportional to the applied load. It should also be noted that there is a non-zero downforce required to initiate polishing. This behavior is consistent with several examples of actual CMP processes where the measured removal rates at low downforce are extremely small or zero.[26] One possible interpretation for this type of behavior would be that a minimum downforce is required for crack initiation and disruption of the protective passivating film on the copper surface.

The ability to simultaneously measure electrochemical behavior with *in situ* mass changes during a polishing experiment is further illustrated in Fig. 7, which depicts polishing results and polarization curves for three different conditions. Polishing experiments were performed on copper at pH 4 (Fig. 7A), at pH 4 with benzotriazole as an inhibiting agent (Fig. 7B), and at pH 12 (Fig. 7C). A summary of the experimental results is given in Table I. At pH 4 in the absence of BTA (Fig. 7A), the frequency response prior to polishing shows a steady increase in magnitude. This increase in frequency reflects a steady loss of material due to a static etching rate of 5 Hz s^{-1}. The frequency increases at $t = 8$ s as the polishing tool contacts the surface. The frequency then decreases at $t = 18$ s when the tool is removed. After polishing, the frequency continues to increase in a steady fashion due to copper etching. Notably, the OCP does not change during polishing, which indicates that the electrode surface is covered with metal throughout the polishing process.

The polishing rate can be determined from this data by first calculating the etching rate and then subtracting that value from the transient data. The polishing rate is then calculated from the frequency change during polishing divided by the polishing time. The value determined for Fig. 7A is 6.7 Hz s^{-1}. This subtraction procedure eliminates the influence of a large etching rate on the accuracy of the calculated polishing rate, which is particularly important for the experiments here, where the contact area between pad and surface is less than the total active electrode area. It should also be noted, that in the solutions studied in this manuscript, the copper etching rates were sufficiently low to minimize the potential of a etching rate overwhelming the measured polishing rate.

Figure 7B depicts a polishing experiment on copper at pH 4 following the addition of 0.1 M BTA. It is well-known that BTA adsorbs on copper and forms a polymeric film, which serves to protect copper from corrosion and etching.[14,27-29] Several differences are seen following the addition of BTA. The OCP increases to a value of −0.32 V, indicating that a passive film has formed. Notably, this open circuit value is sensitive to the history of the electrode and increases to more positive values with growth of a thicker BTA film.[14] The frequency change prior to polishing is also much smaller, which reflects a much lower etching rate for copper with a value of 0.43 Hz s^{-1}, which is conistent with published reports.[30] After contact with the polishing tool at $t = 8$ s, the frequency in-

Downloaded on 2014-05-22 to IP 129.186.176.40 address. Redistribution subject to ECS terms of use (see ecsdl.org/site/terms_use) unless CC License in place (see abstract).

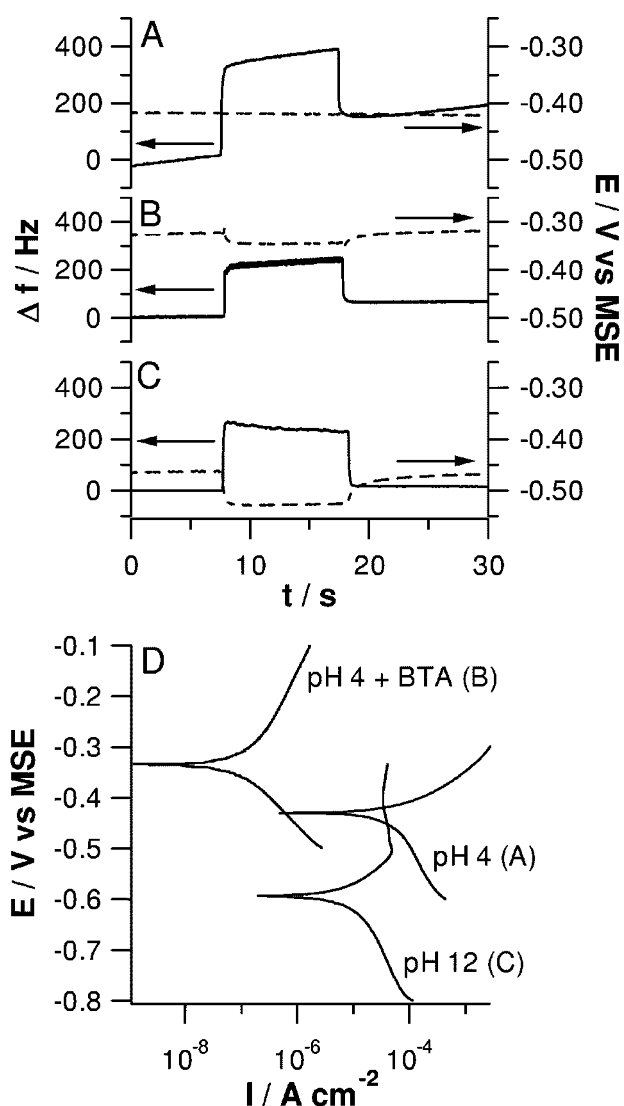

Figure 7. Electrochemical and T-EQCM results for polishing measurements performed in (A) pH 4, (B) pH 4 with BTA, and (C) pH 12. Frequency response (solid line) and OCP (dashed line) are shown. All experiments were performed in 0.1 M Na_2SO_4 with a 10 s polishing step. (D) Polarization curves for copper in solutions depicted in Fig. 7A, B, and C. The scan rate is 10 mV s^{-1}.

creases due to the applied load. Notably, the open circuit decreases during polishing. This is consistent with removal of the passivating BTA layer due to the mechanical action of the polishing pad. After removal of the polishing tool at 18 s, the OCP increases back to the value it had prior to polishing, which suggests reformation of the BTA layer. The frequency response drops and stabilizes after removal of the polishing tool to exhibit a slow etch rate consistent with that seen prior to polishing. The polishing rate as determined

Table I. Summary of polishing data for copper films.

Sample	E_{OC}[a] (V)	ΔE_{OC} (V)	$(\Delta f/\Delta t)_{etch}$ (Hz/s)	$(\Delta f/\Delta t)_{polish}$ (Hz/s)
pH 12	−0.46	−0.063	0.0	1.5
pH 4	−0.42	0.0	5.0	6.7
pH 4 with BTA	−0.32	−0.025	0.43	5.9

[a] As measured prior to polishing experiments.

Table II. Summary of slurry compositions.

% by weight	Slurry 1	Slurry 2	Slurry 3	Slurry 4
Oxidizer				
Ammonum Persulfate			0.7	
H_2O_2	3	3		1
Inhibitor-benzotriazole	0	0.1	0.2	0.005
pH	4	4	10	8
Organic acid-glycine	0.7	0.7	0.5	1
Particle				
Alumina	0.6	0.6		2
Silica			1	

by the frequency response is 5.9 Hz s^{-1}, which is slightly smaller than that observed without BTA. This behavior suggests that the BTA serves to substantially reduce the etching rate of copper due to film formation, but only moderately decreases the polishing rate.[11]

Polishing experiments were also performed on copper in a pH 12 solution (Fig. 7C). At this pH value, the copper film is covered with an oxide layer at OCP. The surface exhibits a negligible etching rate (0.0 Hz s^{-1}) and a relatively low polishing rate (1.5 Hz s^{-1}). The OCP decreases during polishing as the oxide layer is abraded from the surface. The lower polishing rate suggests that the oxide film is mediating the polishing process to slow the removal of material.

Figure 7D depicts polarization curves for copper under the conditions depicted in the polishing experiments. The trends in these curves are consistent with the polishing results as well as previously published reports.[11,17,31,32] Notable features include an OCP that decreases as the pH is raised from 4 to 12. A positive shift in the OCP is also observed upon addition of 0.1 M BTA to the pH 4 solution. However, this shift is a strong function of the electrode history and the thickness of the Cu-BTA film. Other features of these curves have been addressed in the literature.

The results in Fig. 7 and Table I clearly illustrate differences in the electrochemical properties of the copper surface as well as the etching and removal rates as mediated by pH and BTA. The QCM adds the ability to quantitatively measure the rates of material being removed from the copper surface in addition to information gleaned from the changes in OCP.

Further experiments were conducted to evaluate the behavior of complex solution formulations representative of practical slurry chemistries, which contained polishing particles, inhibitor, and oxidizing agent (Table II). Figure 8 depicts T-EQCM results for two different slurry chemistries. Both slurries are in a low pH solution containing alumina particles and peroxide as an oxidizing agent. Slurry 2 contains benzotriazole as an inhibitor while slurry 1 is free of the inhibitor. Very different behavior is observed for the copper response in these systems. Slurry 1 shows a rapid etch rate prior to polishing with a value of 77.2 Hz s^{-1}. In contrast, slurry 2, which contains the inhibitor benzotriazole, exhibits a much lower etch rate of 11.6 Hz s^{-1}. Thus, the protective action of the benzotriazole inhibitor is clearly evident. Differences in the polishing rates are even more substantial. Slurry 1 exhibits a polishing rate of 220 Hz s^{-1} while slurry 2 shows a dramatically lower polishing rate of 4.8 Hz s^{-1}. The rapid etch and polish rates for slurry 1 are expected at these low pH values in the presence of peroxide as an oxidizing agent. The strong inhibiting action of benzotriazole is also evident in the substantial decreases in etch rate and polishing rate for slurry 2.

As indicated in the previous results, the T-EQCM technique allows for detailed, *in situ* analysis of slurry chemistries and the ability to quantitatively assess their influence on etching and polishing behavior. The ability to directly measure mass changes on the copper surface while exposed to different chemical environments also allows one to rapidly quantify the influence of various additives and identify the operative mechanism. Figure 9 depicts the time response of a copper film following the addition of three different slurries to assess how they influence etch rates. The three curves in Fig. 9 reflect different pH and inhibitor concentrations in the presence of a

Downloaded on 2014-05-22 to IP 129.186.176.40 address. Redistribution subject to ECS terms of use (see ecsdl.org/site/terms_use) unless CC License in place (see abstract).

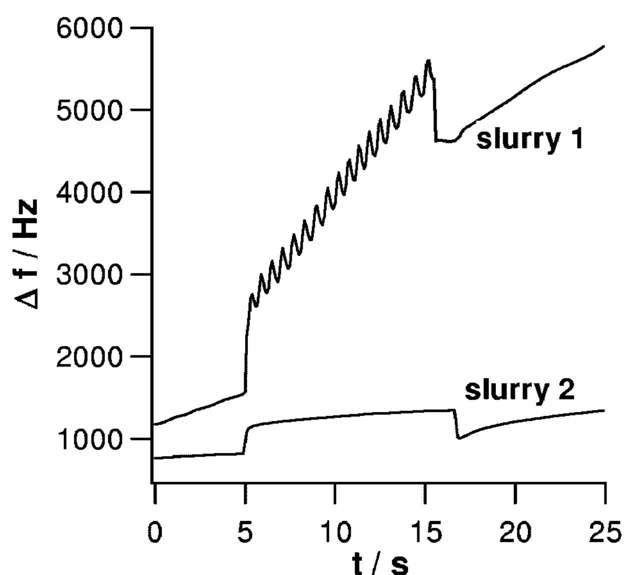

Figure 8. Frequency response of copper film during polishing cycle in two different slurry compositions. Slurries consist of alumina suspension at low pH with peroxide oxidizer. Slurry 2 contains BTA as inhibitor while slurry 1 is absent the inhibitor.

peroxide oxidizer and alumina polishing particles. Slurry 3 is at a high pH and high inhibitor concentration. The increase in mass detected by the crystal frequency response reflects the growth of a relatively thick, passive film on the copper surface. Slurry 4, which corresponds to a high pH and low inhibitor concentration, shows a steady decrease in mass, which is a consequence of a continual etching process that exceeds the formation rate of a protective film. Slurry 2 contains a low pH and high inhibitor concentration and its response depicts an intermediate behavior in which the initial etching is followed by a slow increase in mass corresponding to the formation of a passive film. A comparison of these three response curves provides a rapid method for identifying the action of these slurries and quantify their passivation or etch rates. Slurry 3 exhibits an overall passivating behavior, slurry 4 shows rapid etching, and slurry 2 displays an intermediate response.

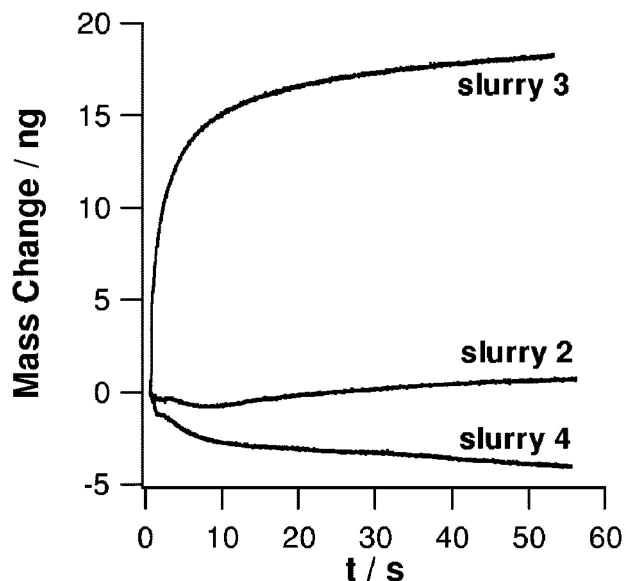

Figure 9. Frequency response during static etching experiment in the presence of three different slurry formulations. The response curves illustrate the change induced by addition of three different slurry chemistries. Slurry 2 contains a high level of BTA at low pH, slurry 3 contains a high level of BTA at high pH, and slurry 4 contains a low level of BTA at high pH. All slurries contain peroxide as an oxidizer.

Conclusions

In summary, this manuscript describes a new technique for the evaluation of the chemical mechanical planarization of metals based upon a combination of the quartz crystal microbalance and a tribo-electrochemical measurement system. This T-EQCM allows simultaneous and *in situ* measurements of electrochemical parameters and mass changes in real time at a metal surface during simulated polishing processes. The quantitative nature of these results allows considerable insight into the subtle surface changes occurring during polishing processes. The results presented illustrate the variety of experiments that can be conducted, including examining the influence of polishing force, measuring etching, and polishing rates *in situ*, and evaluating practical slurry chemistries.

Acknowledgments

The authors would like to acknowledge the National Science Foundation (NSF Career, CTS-9875496) and Cabot Microelectronics, Inc., for partial support of this work. In addition, we thank Vlasta Brusic and Steven Grumbine for helpful comments during the preparation of this manuscript.

Iowa State University assisted in meeting the publication costs of this article.

References

1. M. T. Bohr, *Appl. Surf. Sci.,* **101**, 534 (1996).
2. B. Roberts, A. Harrus, and R. L. Jackson, *Solid State Technol.,* **38**, 69 (1995).
3. P. Wrschka, J. Hernandez, G. S. Oehrlein, and J. King, *J. Electrochem. Soc.,* **147**, 706 (2000).
4. Z. Stavreva, D. Zeidler, M. Plotner, G. Grasshoff, and K. Drescher, *Microelectron. Eng.,* **33**, 249 (1997).
5. R. J. Gutmann, J. M. Steigerwald, L. You, D. T. Price, J. Neirynck, D. J. Duquette, and S. P. Murarka, *Thin Solid Films,* **270**, 596 (1995).
6. Z. Stavreva, D. Zeidler, M. Plotner, and K. Drescher, *Appl. Surf. Sci.,* **91**, 192 (1995).
7. J. Y. Lai, N. Saka, and J. H. Chun, *J. Electrochem. Soc.,* **149**, G41 (2002).
8. Q. Luo and S. V. Babu, *J. Electrochem. Soc.,* **147**, 4639 (2000).
9. F. B. Kaufman, D. B. Thompson, R. E. Broadie, M. A. Jaso, W. L. Guthrie, D. J. Pearson, and M. B. Small, *J. Electrochem. Soc.,* **138**, 3460 (1991).
10. J. M. Steigerwald, S. P. Murarka, J. Ho, R. J. Gutmann, and D. J. Duquette, *J. Vac. Sci. Technol. B,* **13**, 2215 (1995).
11. Q. Luo, D. R. Campbell, and S. V. Babu, *Thin Solid Films,* **311**, 177 (1997).
12. U. Bertocci and D. Turner, in *Encyclopedia of Electrochemistry of the Elements*, A. J. Bard, Editor, Marcel Dekker, New York (1974).
13. J. van Muylder, in *Comprehensive Treatise of Electrochemistry*, J. M. Bockris, B. E. Conway, E. Yeager, and R. White, p. 23, Plenum Press, New York (1981).
14. V. Brusic, M. A. Frisch, B. N. Eldridge, F. P. Novak, F. B. Kaufman, B. M. Rush, and G. S. Frankel, *J. Electrochem. Soc.,* **138**, 2253 (1991).
15. Q. Luo, R. A. Mackay, and S. V. Babu, *Chem. Mater.,* **9**, 2101 (1997).
16. Z. Stavreva, D. Zeidler, M. Plotner, and K. Drescher, *Appl. Surf. Sci.,* **108**, 39 (1997).
17. S. Aksu and F. M. Doyle, *J. Electrochem. Soc.,* **149**, G352 (2002).
18. J. Y. Lai, N. Saka, and J. H. Chun, *J. Electrochem. Soc.,* **149**, G31 (2002).
19. S. Tamilmani, W. Huang, S. Raghavan, and R. Small, *J. Electrochem. Soc.,* **149**, G638 (2002).
20. S. Seal, S. C. Kuiry, and B. Heinmen, *Thin Solid Films,* **423**, 243 (2003).
21. J. M. Steigerwald, D. J. Duquette, S. P. Murarka, and R. J. Gutmann, *J. Electrochem. Soc.,* **142**, 2379 (1995).
22. D. A. Buttry and M. D. Ward, *Chem. Rev. (Washington, D.C.),* **92**, 1355 (1992).
23. M. D. Ward and D. A. Buttry, *Science,* **249**, 1000 (1990).
24. B. A. Martin and H. E. Hager, *J. Appl. Phys.,* **65**, 2630 (1989).
25. F. Preston, *J. Soc. Glass Technol.,* **11**, 214 (1927).
26. D. Stein, in *Springer Series in Materials Science*, M. R. Oliver, Editor, p. 425, Springer-Verlag, New York (2004).
27. W. Qafsaoui, C. Blanc, N. Pebere, H. Takenouti, A. Srhiri, and G. Mankowski, *Electrochim. Acta,* **47**, 4339 (2002).
28. A. T. Al-Hinai and K. Osseo-Asare, *Electrochem. Solid-State Lett.,* **6**, B23 (2003).
29. M. Hepel and E. Cateforis, *Electrochim. Acta,* **46**, 3801 (2001).
30. M. T. Wang, M. S. Tsai, C. Liu, W. T. Tseng, T. C. Chang, L. J. Chen, and M. C. Cheng, *Thin Solid Films,* **308**, 518 (1997).
31. Y. Ein-Eli, E. Abelev, and D. Starosvetsky, *J. Electrochem. Soc.,* **151**, G236 (2004).
32. Y. Ein-Eli, E. Abelev, and D. Starosvetsky, *Electrochim. Acta,* **49**, 1499 (2004).

Downloaded on 2014-05-22 to IP 129.186.176.40 address. Redistribution subject to ECS terms of use (see ecsdl.org/site/terms_use) unless CC License in place (see abstract).